



Synthesis, Antimicrobial Activity and Molecular Docking of Some Novel 2-Aryl-4H-[1,3]-thiazolo[4,5-b]indoles

BHARGAVI POSINASETTY^{1,2,✉}, RAJASEKHAR KOMARLA KUMARACHARI^{3,*✉}, PRASHANTI CHITRAPU^{4,✉},
JYOTHIRMAYEE DEVINENI^{5,✉}, SUDHAHAR DHARMALINGAM^{6,✉}, CHILAMAKURU NARESH BABU^{7,✉} and JAYENDRA KUMAR^{8,✉}

¹Department of Public Health, University of Southern Mississippi, MS-39406, USA

²Department of Dentistry, Government Dental College and Research Institute, Bellary-583104, India

³Department of Pharmaceutical Chemistry, Sri Padmavathi School of Pharmacy, Tiruchanur, Tirupati-517503, India

⁴Vision College of Pharmaceutical Sciences and Research, Secunderabad-500092, India

⁵Department of Pharmaceutics and Biotechnology, KVSR Siddhartha College of Pharmaceutical Sciences, Vijayawada-520010, India

⁶Department of Pharmaceutical Chemistry and Analysis, Nehru College of Pharmacy, Thiruvilwamala-680588, India

⁷Raghavendra Institute of Pharmaceutical Education and Research, Ananthapuramu-515721, India

⁸SRM Modinagar College of Pharmacy, SRM Institute of Science and Technology Delhi-NCR Campus, Ghaziabad-201204, India

*Corresponding author: Fax: +91 877 2237732; E-mail: komarla.research@gmail.com

Received: 30 November 2023;

Accepted: 30 December 2023;

Published online: 31 January 2024;

AJC-21526

In present study, six novel 2-aryl-4H-[1,3]-thiazolo[4,5-b]indoles (**4a-f**) were synthesized by integrating thiazole and indole motifs through a three-component one-pot condensation involving isatin, ammonium thiocyanate and arylaldehydes. Structural confirmation was achieved using IR, ¹H NMR and mass spectrometric techniques. Molecular targets, bioactivity scores, drug-likeness, anti-tuberculosis and antibacterial properties and toxicity were all predicted using various computational techniques. To calculate binding affinities to *Mycobacterium tuberculosis* enoyl-ACP reductase and *Escherichia coli* Topoisomerase IV, *in vitro* bioactivity studies were performed and Schrödinger docking simulations were performed. Anti-tubercular efficacy was evaluated using the MABA method, while antibacterial effectiveness against both Gram-positive and Gram-negative bacteria was assessed through the agar plate method. The results highlight the potential of these heterocyclic molecular hybrids, positioning them as promising candidates for further lead optimization in the development of more potent and safer pharmaceutical agents.

Keywords: Thiazolo[4,5-b]indoles, Toxicity, Antimicrobial activity, Molecular docking.

INTRODUCTION

The synthesis and exploration of heterocyclic compounds have been integral to the field of medicinal chemistry, offering diverse scaffolds with unique physico-chemical and biological properties. Among these, the thiazolo-indole scaffold has garnered significant attention due to its versatile chemistry and promising biological activities [1,2]. The thiazole ring, a five-membered heterocycle containing both sulfur and nitrogen, is known for its ability to impart desirable pharmacological properties to organic compounds. When incorporated into indole derivatives, this combination not only introduces structural diversity but also often results in compounds with enhanced bioactivity. The 2-aryl-4H-[1,3]thiazolo[4,5-b]indoles represent

a class of compounds that hold great potential for the medicinal applications, unveiling a balance between synthetic accessibility and biological relevance [3-5].

The significance of thiazolo indoles in medicinal chemistry arises from their reported activities in various therapeutic areas, including antimicrobial, anti-inflammatory and anticancer properties [6-8]. Additionally, the ability of these compounds to interact with specific biological targets has sparked interest in exploring their potential as lead compounds for drug development [9-13]. In an urgent quest for novel and effective drugs, especially in the context of tuberculosis and bacterial infections in SARS-CoV-2 (COVID-19), the investigation of thiazolo-indoles emerges as a promising avenue for discovering potent antitubercular agents [14]. These compounds, characterized by the fusion of

thiazole and indole rings, represent an exciting prospect in the development of drugs capable of addressing bacterial infections associated with both tuberculosis and SARS-CoV-2. The need for new medicinal treatments highlights the importance of investigating various chemical structures, and thiazolo indoles emerge as potentially valuable contenders in this endeavor [15-17].

The synthesis of these compounds involves a strategic combination of the synthetic methodologies to ensure the structural diversity while maintaining the synthetic feasibility. The resulting library of 2-aryl-4H-[1,3]-thiazolo[4,5-*b*]indoles serves as a platform for investigating the structure-activity relationship and optimizing the pharmacological potential of this molecular scaffold [18,19].

In this comprehensive study, we aim to elucidate the chemistry and pharmacological significance of 2-aryl-4H-[1,3]thiazolo[4,5-*b*]indoles, specifically in the context of their antitubercular and antibacterial activities. By employing a synergistic methodology that combines organic synthesis, biological evaluation, and molecular docking investigations, the main objective is to provide significant insights that may assist in the advancement of novel treatment approaches to combat multidrug resistant tuberculosis and bacterial infections.

EXPERIMENTAL

All chemicals employed in this study were sourced from Sigma-Aldrich Co. (St. Louis, USA), Merck (Whitehouse Station, NJ, USA), Qualigens Fine Chemicals (Mumbai, India), Loba Chemie Pvt. Ltd (Mumbai, India) and Himedia Lab. Pvt. Ltd (Mumbai, India).

To determine the melting points of the synthesized compounds, a digital melting point apparatus with open capillary tubes was utilized. The reported values are presented without correction. Compound purity was assessed through thin-layer chromatography, using pre-coated silica gel strips and a solvent system comprising a 2:1 ratio of hexane to ethyl acetate. Chromatographic spots were visualized using an ultraviolet chamber.

Infrared spectra (expressed in ν/cm) were recorded using a Shimadzu FT-IR 4000 instrument equipped with KBr disks. CHNO elemental analysis was executed using the Perkin-Elmer Series II 2400 CHNS/O elemental analyzer. Mass spectra were obtained *via* a JEOL GC mate II GC-Mass spectrometer, oper-

ating at 70 eV and utilizing the direct insertion probe method. For NMR spectra, a BRUKER AVIII-500 MHz FT NMR spectrometer was used, with tetramethylsilane as the internal standard and DMSO as the preferred solvent.

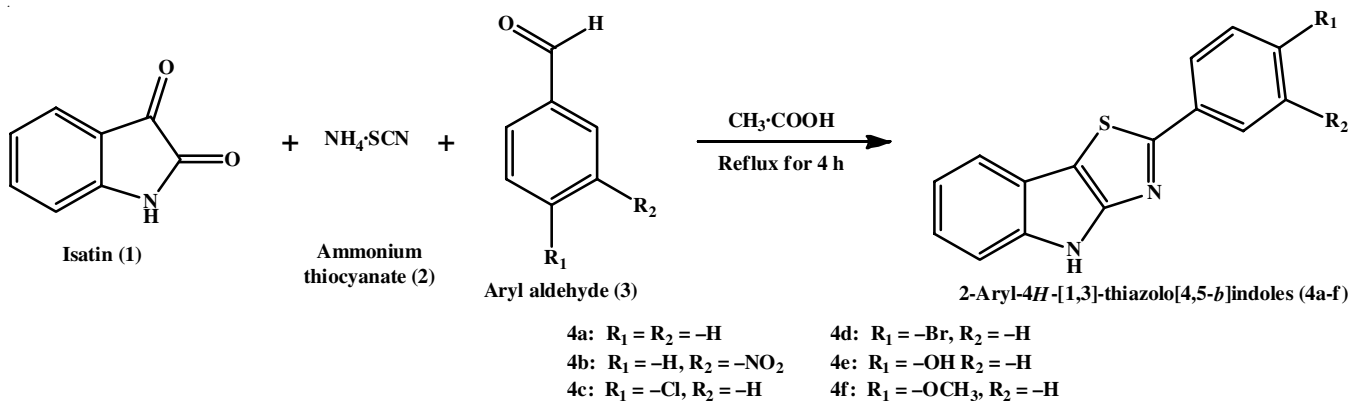
Synthesis of 2-aryl-4H-[1,3]-thiazolo[4,5-*b*]indoles (4a-f):

A mixture consisting of 0.25 mol of isatin, 0.25 mol of aryl aldehyde and 10 g of ammonium thiocyanate was placed in a 250 mL round bottomed flask. The reaction mixture was refluxed with 100 mL of glacial acetic acid for 4 h. Subsequently, the resulting mixture was left overnight and then filtered to remove any formed precipitate. Following this, 250 mL of distilled water was added to the filtrate and stirred thoroughly to facilitate the washing of product with distilled water. The precipitate formed after rinsed with distilled water was collected, and the resulting filtrate was neutralized by adding NH_4OH in order to extract the second portion of solid. Then, both solid products were combined, thoroughly dried and the obtained product underwent recrystallization from methanol (**Scheme-I**). The homogeneity and purity of the compound were confirmed through TLC on silica gel plates using a hexane:ethyl acetate solvent system.

2-Phenyl-4H-[1,3]thiazolo[4,5-*b*]indole (4a): Yield: 65%; m.p.: 146-149 °C; FT-IR (KBr, ν_{max} , cm^{-1}): 3428 (N-H), 1604 (C=C), 1660 (C=N); ^1H NMR (DMSO- d_6 , δ ppm): 7.18-7.35 (2H, 7.25 (d), 7.29 (t)), 7.43-7.61 (3H, 7.49 (t), 7.54 (d)), 7.63-7.82 (2H, 7.70 (d), 7.76 (d)), 8.09 (2H, d); MS (m/z , %): 250.05 (M^+). Anal. calcd. (found) % for $\text{C}_{15}\text{H}_{10}\text{N}_2\text{S}$: C, 71.97 (72.04); H, 4.03 (3.98); N, 11.19 (11.21); S, 12.81 (12.85).

2-(3-Nitrophenyl)-4H-[1,3]thiazolo[4,5-*b*]indole (4b): Yield: 72%; m.p.: 206-209 °C; FT-IR (KBr, ν_{max} , cm^{-1}): 3382 (N-H), 1612 (C=C), 1437(N-O), 1656 (C=N); ^1H NMR (DMSO- d_6 , δ ppm): 6.86 (1H, d), 7.39-7.61 (4H, 7.46 (d), 7.48 (d), 7.52 (d), 7.54 (d)), 7.68-7.87 (3H, 7.74 (d), 7.74 (t), 7.80 (d)); MS (m/z , %): 295.04 (M^+). Anal. calcd. (found) % for $\text{C}_{15}\text{H}_9\text{N}_3\text{O}_2\text{S}$: C, 61.01 (61.07); H, 3.07 (3.10); N, 14.23 (14.20); O, 10.84 (10.86); S, 10.86 (10.91).

2-(4-Chlorophenyl)-4H-[1,3]thiazolo[4,5-*b*]indole (4c): Yield: 68%; m.p.: 129-132 °C; FT-IR (KBr, ν_{max} , cm^{-1}): 3307 (N-H), 1602 (C=C), 1639 (C=N) 804 (C-Cl); ^1H NMR (DMSO- d_6 , δ ppm): 7.16-7.31 (2H, 7.22 (t), 7.24 (d)), 7.62-7.90 (6H, 7.68 (d), 7.71 (d), 7.74 (d), 7.83 (d)); MS (m/z , %): 284.01 (M^+). Anal. calcd. (found) % for $\text{C}_{15}\text{H}_9\text{N}_2\text{S}\text{Cl}$: C, 63.27 (63.31); H, 3.19 (3.22); N, 9.84 (9.88); S, 11.26 (11.24); Cl, 12.45 (12.62).



Scheme-I

2-(4-Bromophenyl)-4H-[1,3]thiazolo[4,5-*b*]indole (4d):

Yield: 65%; m.p.: 192-194 °C; FT-IR (KBr, ν_{\max} , cm^{-1}): 3346 (N-H), 1608 (C=C), 1656 (C=N) 574 (C-Br); $^1\text{H NMR}$ (DMSO- d_6 , δ ppm): 7.14-7.28 (2H, 7.21 (d), 7.22 (t)), 7.60-7.89 (6H, 7.66 (d), 7.68 (d), 7.71 (d), 7.83 (d)); MS (m/z , %): 327.96 (M^+). Anal. calcd. (found) % for $\text{C}_{15}\text{H}_9\text{N}_2\text{SBr}$: C, 54.72 (54.76); H, 2.76 (2.79); N, 8.51 (8.48); S, 9.74 (9.77); Br, 24.27 (24.30).

4-(4H-[1,3]thiazolo[4,5-*b*]indol-2-yl)phenol (4e):

Yield: 74%; m.p.: 182-184 °C; FT-IR (KBr, ν_{\max} , cm^{-1}): 3457 (N-H), 1624 (C=C), 1662 (C=N), 3204 (O-H); $^1\text{H NMR}$ (DMSO- d_6 , δ ppm): 7.26 (2H, d), 7.35-7.50 (2H, 7.42 (d), 7.44 (t)), 7.59-7.80 (4H, 7.65 (d), 7.72 (d), 7.74 (d)); MS (m/z , %): 266.05 (M^+). Anal. calcd. (found) % for $\text{C}_{15}\text{H}_{10}\text{N}_2\text{OS}$: C, 67.65 (67.68); H, 3.78 (3.81); N, 10.52 (10.55); O, 6.01 (6.08); S, 12.04 (12.07).

2-(4-Methoxyphenyl)-4H-[1,3]thiazolo[4,5-*b*]indole

(4f): Yield: 75%; m.p.: 161-163 °C; FT-IR (KBr, ν_{\max} , cm^{-1}): 3298 (N-H), 1612 (C=C), 1658 (C=N), 1168 (C-O); $^1\text{H NMR}$ (DMSO- d_6 , δ ppm): 3.87 (3H, s), 7.19 (2H, d), 7.34-7.52 (2H, 7.41 (d), 7.45 (d)), 7.64-7.87 (4H, 7.70 (d), 7.71 (d), 7.80 (d)); MS (m/z , %): 280.06 (M^+). Anal. calcd. (found) % for $\text{C}_{16}\text{H}_{12}\text{N}_2\text{OS}$: C, 68.55 (68.61); H, 4.31 (4.34); N, 9.99 (9.94); O, 5.71 (5.75); S, 11.44 (11.47).

In silico profile

Prediction of biological activity: The pharmacological activity prediction of the titled compounds was done using the PASS online program. By comparing the structures of the synthesized compounds to those of known biologically active chemicals, this prediction algorithm may assess their structures and indicate prospective pharmacological qualities that can be confirmed in future experiments. The database of PASS, which includes thousands of chemicals from the training set, allows for a more objective assessment of possible biological activities. Even for initial studies, PASS software is helpful since it simply requires the structural formula or SMILES notation of the chemical molecule [20].

After submitting the structures of the title compounds to the PASS online tool, the analysis generated predictions regarding multiple probable modes of action and biological activities. The compounds showed a propensity for activity as antitubercular and antibacterial agents, in addition to other biologically significant activities.

Molinspiration: Molinspiration stands as a valuable resource for the computational chemistry community, offering free online services to predict bioactivity scores associated with critical drug targets. These targets span a broad spectrum, ranging from G protein-coupled receptor (GPCR) ligands to kinase inhibitors, ion channel modulators, enzymes and nuclear receptors. Molinspiration's user-friendly and easily accessible platform plays a crucial role in supporting the research efforts of the computational chemistry community, streamlining the exploration of molecular properties and bioactivity predictions for a diverse range of chemical compounds [21].

Osiris property explorer: The Osiris property explorer is a crucial component of Actelion's internal substance registration system. Users are enabled to draw chemical structures

and, once verified, the system does immediate calculations of crucial properties for drugs development. The prediction findings are presented with given numerical values and colour codes, making it easier to interpret.

Properties linked to a higher probability of undesirable outcomes, such as mutagenicity, are clearly emphasized in red, attracting attention to the possible issues. In contrast, qualities that indicate drug-like behavior are depicted in green, indicating favorable attributes for drug development. The utilization of colour-coded presentations greatly facilitates the rapid identification of compounds with favourable characteristics and possible drawbacks, hence optimizing the efficiency of the drug discovery and development process [22].

Swiss ADME: The physico-chemical qualities, lipophilicity, water solubility, lipophilicity, pharmacokinetics, drug likeness, molecular target and medicinal chemistry parameters were among the parameters evaluated using the prediction tools of the Swiss ADME online platform. The drug-likeness of the compounds (**4a-e**) was evaluated by doing *in silico* ADMET (absorption, distribution, metabolism, excretion and toxicity) predictions using the SwissADME software for the chemical set [23].

Molecular docking studies

Preparation of target molecules: The target molecules were prepared using the GLIDE docking tool (Schrodinger 2020-1) [24] in a dual-target docking investigation. The six synthesized compounds were docked within the active sites of two crystal structures *viz.* the enoyl-ACP reductase from *Mycobacterium tuberculosis* enoyl (PDB code: 2PR2) and Escherichia coli topoisomerase IV ParE 24kDa subunit (PDB code: 1S14).

A number of tools, including as ERRAT, Verify 3D and the structural analysis and verification server, were used to carefully evaluate the quality of the target protein structures [25-27]. The results of these evaluations proved that all of the protein models were of good quality and acceptable. In addition, the Ramachandran plot was thoroughly analyzed using RAMPAGE to assess the dihedral angles and allowable conformations [28].

Preparation of ligand molecules: The 2D chemical structures of compounds **4a-f** were initially generated and saved in binary format using ChemDraw Ultra Version 8.0.3 [29] during the ligand molecule preparation. With the help of Open Babel GUI version 2.4.1, these structures were subsequently adapted to sdf format. The structures were transformed for further use in the study process with the help of Open Babel, a flexible virtual screening tool made for Windows [30,31].

After that, the OPLS3e force field with Ligprep was used to perform comprehensive energy minimization. Ionization at a target pH of 7.0 ± 2.0 , dehydrating and the preservation of specific chiralities were all factors in this procedure [32]. By using adenosine triphosphate (ATP) as a reference ligand in the docking assays, binding affinities could be more easily compared. Binding interactions and docking scores generated from GLIDE SP ligand docking were also carefully examined to evaluate the obtained results.

Antimicrobial activity

Antitubercular activity: Using the microplate Alamar blue assay method (MABA), the antitubercular activity of the synthesized derivatives, namely 2-aryl-4*H*-[1,3]thiazolo[4,5-*b*]indoles (**4a-f**), was examined. Experiments were conducted on *M. tuberculosis* H37 RV strain using each of the synthetic compounds, with isonicotinic acid hydrazide (INH) served as the reference drug.

To prevent medium evaporation during incubation, 200 μ L of sterile deionized water was added to the outermost wells of a sterile 96-well plate in this experiment. Afterward, 100 μ L of Middlebrook 7H9 (MB 7H9) broth was gently poured into the wells, and the synthesized compounds were then diluted in a sequential manner directly on the plate. The compounds were evaluated for their antitubercular activity at different concentration of doses ranging from 0.2 to 100 μ g/mL.

The plates were placed in an incubator set at 37 °C for 5 days after being covered and parafilm. To each well, 25 mL of a freshly made 1:1 mixture of Alamar blue reagent and 10% Tween 80 was added after the incubation period. The plates were kept in the incubator for a further 24 h. The interpretation of the results was based on the colour change observed in the wells *viz.* a blue colour indicated no bacterial growth, while a pink colour signified bacterial growth [33].

Antibacterial activity: The agar cup plate method was used to evaluate the antibacterial activity of the synthesized compounds (**4a-f**). These compounds were investigated in relation to several bacterial species including Gram-negative (*Escherichia coli* and *Pseudomonas aeruginosa*) and Gram-positive (*Bacillus subtilis* and *Staphylococcus epidermatitis*). The minimum inhibitory concentration (MIC) method was employed for assessment with ciprofloxacin used as a reference standard.

Brain heart infusion agar was allowed to attain room temperature during the procedure. The colonies were subsequently put onto the plates and their turbidity was visually adjusted using broth in order to achieve the same level of turbidity as 0.5 McFarland turbidity standard that had been vortexed. To ensure evenly distribution, the agar plate was swabbed three times, with each swabbing, the plates were rotated about 60°. Following this step, the contaminated sample plate was left undisturbed for at least 5 min before the drugs were administered.

After pressing a heated, 5 mm hollow tube into the inoculated agar plate, five wells were developed; and the tubes were then quickly withdrawn. Then, the synthesized compounds were introduced to the corresponding wells on each plate in volumes of 75, 50, 25, 10 and 5 μ L, respectively. After the chemical was applied, the plates were incubated for 15 min and kept in an incubator at 37 °C for 24 h. Each synthesized compound underwent repeated dilution up to a 10⁻⁹ dilution as part of the MIC method [34,35].

RESULTS AND DISCUSSION

The synthetic pathway, outlining the present approach to synthesize the title compounds, is depicted in **Scheme-I**. The successful synthesis and characterization of 2-aryl-4*H*-[1,3]-thiazolo[4,5-*b*]indoles (**4a-f**) were accomplished through the

reaction of isatin (**1**) with ammonium thiocyanate (**2**) and aryl-aldehydes (**3**) resulting in cyclization and the formation of a thiazole ring. The purity of all the synthesized compounds was validated through thin-layer chromatography (TLC) utilizing a mobile phase composed of a hexane and ethyl acetate mixture. Additionally, all the synthesized compounds demonstrated distinctive peaks in both FT-IR and NMR spectra. Mass spectra analysis confirmed the presence of the expected molecular ion peak (*M*⁺) fragments for the synthesized compounds.

In silico profiling: Table-1 presents the expected biological activity as predicted by the PASS computational tool. PASS employs an exhaustive study of structure-activity connections, extracting knowledge from a comprehensive training dataset of around 60,000 molecules with biological activity. This dataset encompasses around 4500 unique categories of biological activities. The computed probabilities (Pa and Pi) offer a prediction of the probability of specific compounds exhibiting distinct biological activities.

TABLE-1
PREDICTED BIOLOGICAL ACTIVITY SPECTRUM
OF SYNTHESIZED COMPOUNDS **4a-f**

Compd.	Pa	Pi	Activity
4a	0.827	0.005	Cardiotonic
	0.629	0.004	Male reproductive dysfunction treatment
	0.584	0.061	Anti-neoplastic (brain cancer)
	0.390	0.035	Anti-tubercular
4b	0.758	0.005	Cardiotonic
	0.578	0.005	Male reproductive dysfunction treatment
	0.483	0.014	Anti-tubercular
	0.458	0.117	Anti-neoplastic (brain cancer)
4c	0.730	0.007	Cardiotonic
	0.592	0.005	Male reproductive dysfunction treatment
	0.533	0.080	Anti-neoplastic (brain cancer)
	0.365	0.042	Anti-tubercular
4d	0.708	0.008	Cardiotonic
	0.590	0.005	Male reproductive dysfunction treatment
	0.434	0.023	Anti-tubercular
	0.443	0.128	Anti-neoplastic (brain cancer)
4e	0.728	0.007	Cardiotonic
	0.588	0.060	Anti-neoplastic (brain cancer)
	0.570	0.005	Male reproductive dysfunction treatment
	0.398	0.033	Anti-tubercular
4f	0.771	0.005	Cardiotonic activity
	0.662	0.040	Anti-neoplastic (brain cancer)
	0.593	0.005	Male reproductive dysfunction treatment
	0.395	0.034	Anti-tubercular
INH	0.810	0.003	Antituberculosic
	0.798	0.004	Antimycobacterial
	0.371	0.038	Antibacterial
	0.226	0.042	<i>trans</i> -2-Enoyl-CoA reductase (NAD+) inhibitor
Cipro-floxacin	0.639	0.008	Antimycobacterial
	0.588	0.009	Antibacterial
	0.452	0.019	Antituberculosic
	0.304	0.086	Antiviral (Adenovirus)

Interestingly, all the produced compounds were anticipated to have antitubercular activity, as evidenced by Pa values < 0.5. However, in contrast to this hypothesis, the actual evaluation showed that all of these drugs displayed substantial anti-

tubercular action. This result contradicts the initial prediction made by the PASS software.

Molinspiration technique was utilized in order to make predictions regarding the bioactivity scores of each of the synthesized compounds as shown in Fig. 1. Notably, compound **4e** emerged as a standout candidate among the synthesized compounds revealing the substantial bioactivity values. These findings emphasize the potential of this compound as a kinase inhibitor and enzyme inhibitor.

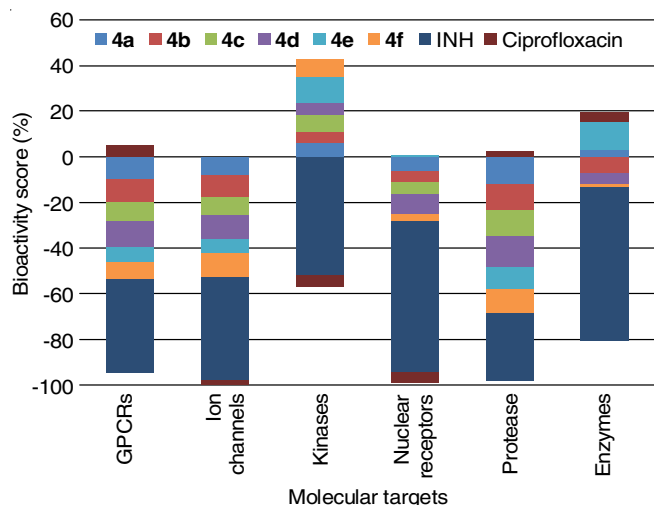


Fig. 1. Calculation of bioactivity scores using molinspiration

The toxicological characteristics and drug score values projected by the Osiris property explorer are presented in Table-2. Promisingly, among the synthesized compounds, it was anticipated that five of them demonstrated a favorable safety profile in terms of toxicity, as shown by their projected drug score values. Compound **4b** was projected to demonstrate mutagenicity, similar to the standard drug isoniazid commonly employed in *in vitro* investigations.

Table-3 summarizes the physico-chemical, pharmacokinetic and medicinal chemistry properties predicted by Swiss ADMET. All the synthesized compounds adhere to Lipinski's rule, meeting criteria for drug-likeness, with parameters such as molecular weight, Clog P (lipophilicity) and counts of hydrogen bond donors and acceptors within acceptable limits.

The results in Table-3 highlight that all the compounds demonstrate high gastrointestinal absorption, blood-brain barrier permeability and no skin permeation or pan assay interference structural alerts (PAINS). Furthermore, no compounds are predicted as P-glycoprotein substrates, as validated with a support vector machine (SVM) model. The use of 1024 fragmental contributions (FP2) predicts that compounds **4a-f** can be easily synthesized, aligning well with the observed yields.

Molecular docking studies: The quality of the 3D models for the target molecules was evaluated using Ramachandran plot calculations conducted *via* RAMPAGE. For 2PR2, 89.8% of residues fell within the favored region, 8.9% in the allowed region and 0.9% in the outlier region. In the case of 1S14, these values were 94.6%, 5.4% and 0%, respectively. These percentages, nearing 100%, signify outstanding model quality, confirming the high caliber of the predicted models (Fig. 2).

Furthermore, these protein models underwent validation using other servers, including ERRAT and verify 3D. ERRAT analysis yielded overall quality factors of 94.21% for 2PR2 and 95.83% for 1S14, surpassing the 95% rejection limit and confirming the quality of the target protein models. Verify 3D analysis revealed that all amino acids in 2PR2 received non-negative scores, while a few residues in 1S14 had marginally negative scores. Additionally, 99.25% of amino acid residues in 2PR2 and 46.43% in 1S14 exhibited 3D-1D scores greater than or equal to 0.2, indicating a structurally acceptable environment (Fig. 3).

Glide, a popular Schrödinger docking program, was used to predict docking scores for each ligand with respect to both target proteins. As shown in Figs. 4 and 5, the two target protein

TABLE-2
PREDICTIVE TOXICITY PROPERTIES USING OSIRIS MOLECULAR PROPERTY EXPLORER

Compound	Drug likeness	Drug score	Mutagenicity	Tumorigenicity	Irritant	Reproductive toxicity
4a	-0.91	0.41	No	No	No	No
4b	-6.97	0.24	YES	No	No	No
4c	0.16	0.39	No	No	No	No
4d	-3.47	0.25	No	No	No	No
4e	-0.97	0.44	No	No	No	No
4f	-1.62	0.37	No	No	No	No
INH	-5.06	0.06	YES	YES	YES	YES
Ciprofloxacin	2.07	0.89	No	No	No	No

TABLE-3
PREDICTION OF PHARMACOKINETIC AND MEDICINAL CHEMISTRY PROPERTIES USING SWISS ADME

Compound	GIA	BBBP	P-gpS	LogKp (cm/s)	BAS	PAINS alert	SA
4a	High	Yes	Yes	-4.63	0.55	0	2.59
4b	High	No	No	-5.03	0.55	0	2.69
4c	High	Yes	Yes	-4.39	0.55	0	2.60
4d	High	Yes	Yes	-4.62	0.55	0	2.63
4e	High	No	Yes	-4.98	0.55	0	2.57
4f	High	Yes	Yes	-4.84	0.55	0	2.64
INH	High	No	No	-7.63	0.55	0	1.23
Ciprofloxacin	High	No	Yes	-8.53	0.55	0	3.22

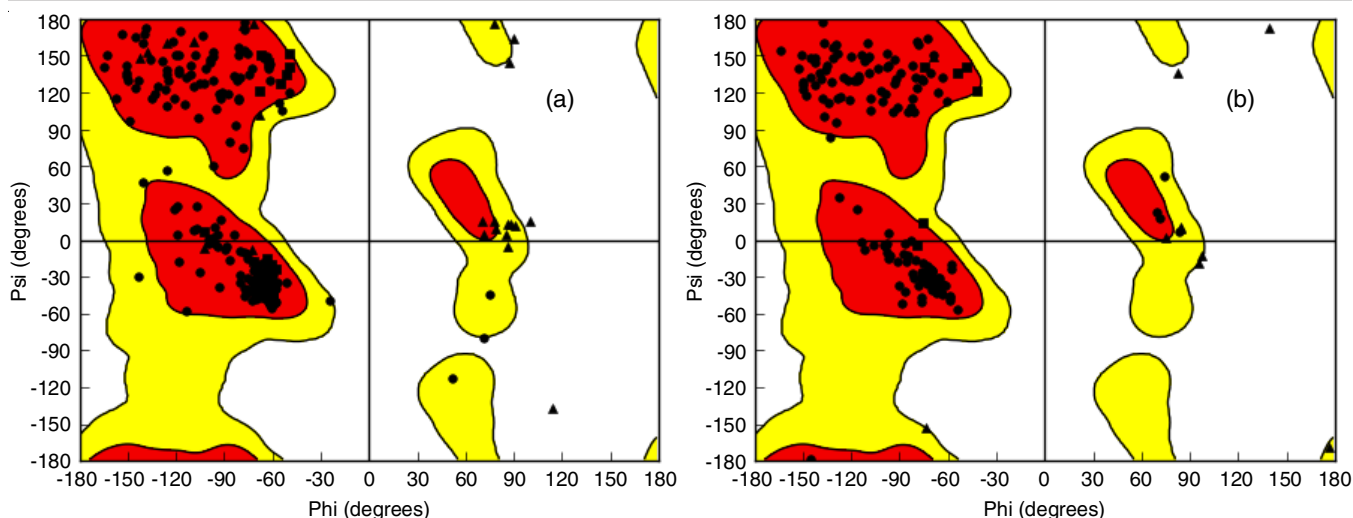


Fig. 2. Ramachandran plots generated *via* RAMPAGE for (a) 2PR2 and (b) 1S14; Residues in favoured (red), allowed (yellow) and outlier regions (white)

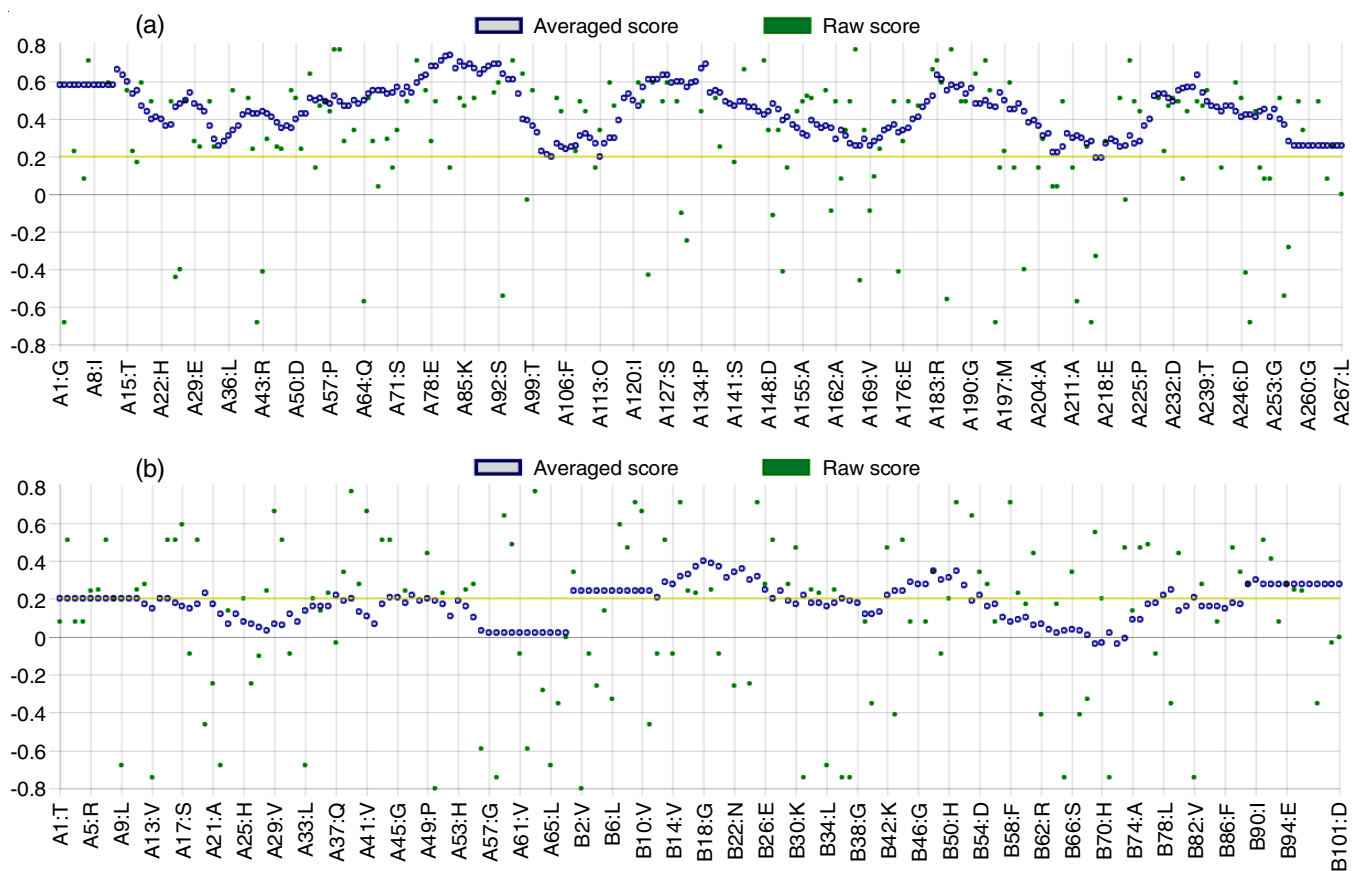


Fig. 3. Verify 3D results of (a) 2PR2 and (b) 1S14

models were docked with compounds **4a-f**. Ten binding poses were generated for each docking process, and the highest score was chosen. Among the synthesized compounds, **4d** and **4b** docked best against 2PR2 and 1S14, respectively. All compounds demonstrated promising docking scores comparable to their respective standards.

Tables 4 and 5 present a summary of the hydrogen bonding and ionic interactions between the synthesized compounds (**4a-f**) and the amino acid residues of target proteins 2PR2 and 1S14.

All the synthesized compounds displayed both hydrogen bonding and ionic interactions with 2PR2. Additionally, these compounds exhibited hydrogen bonding interactions akin to the standard drug INH (GLY 96), though at different interaction sites (GLY 192). The discovery that synthesized compound **4b** exhibited an ionic interaction (GLU 1046), distinct from both the standard and other synthesized compounds, introduces an intriguing aspect. In contrast, the remaining synthesized compounds lacked an ionic interaction but displayed variations

TABLE-4
DOCKING SCORE AND MOLECULAR INTERACTION OF
SYNTHESIZED COMPOUNDS WITH 2PR2 PROTEIN

Compound	Docking score	H-Bond interactions	Ionic interactions
4a	-8.60850	GLY192	PHE149
4b	-8.48537	ILE21, GLY192	PHE149
4c	-8.66031	GLY192	PHE149
4d	-8.37364	GLY192	PHE149
4e	-9.02152	SER94, GLY192	PHE149, LYS165
4f	-8.93187	GLY192	PHE149
Isoniazid	-7.24400	VAL 95, GLY 96	–

TABLE-5
DOCKING SCORE AND MOLECULAR INTERACTION OF
SYNTHESIZED COMPOUNDS WITH 1S14 PROTEIN

Compound	Docking score	H-Bond interactions	Ionic interactions
4a	-4.93082	VAL1039	–
4b	-4.24938	VAL1039	GLU1046
4c	-5.18085	VAL1039	–
4d	-5.09742	VAL1039	–
4e	-5.09934	VAL1039	–
4f	-4.8203	VAL1039	–
Ciprofloxacin	-6.02035	ASP 1069, GLY 1073	–

from the standard concerning hydrogen bonding interaction sites.

Antimicrobial activity: The antitubercular activity of the synthesized thiazolo indole hybrids (**4a-f**) was evaluated against *Mycobacterium tuberculosis* H37Rv in Middlebrook 7H9 broth media (MB 7H9 broth), with isoniazid (INH) as the standard drug. The screening results (Table-6) indicated that compounds **4e** and **4f**, having a *p*-hydroxy and *p*-methoxy group, respectively, on the aromatic moiety at the 2nd position of thiazole ring, exhibited activity at concentrations of 25, 50 and 100 µg/mL. However, the rest of compounds showed no significant activity at concentrations below 50 µg/mL. Notably, all the synthesized compounds were inactive at concentrations under 25 µg/mL compared to the standard drug INH.

TABLE-6
ANTI-TUBERCULAR ACTIVITY OF
SYNTHESIZED COMPOUNDS **4a-f**

Compound	Minimum inhibitory concentration		
	25 µg/mL	50 µg/mL	100 µg/mL
4a	R	S	S
4b	R	S	S
4c	R	S	S
4d	R	S	S
4e	S	S	S
4f	S	S	S
INH	S	S	S

The agar cup-plate method was employed to evaluate the antibacterial activity of all synthesized compounds (**4a-f**), with ciprofloxacin used as reference standard. Notably, significant antibacterial activity was observed at a dose level of 100 µg, as shown in Fig. 6. Compounds **4c** and **4d** exhibited the highest activity among all the tested bacterial strains, likely due to the

presence of distinct electronically active groups, specifically the *p*-chloro and *p*-bromo groups present on the phenyl ring at the 2nd position of thiazole. In addition, all the compounds exhibited significant antibacterial activity against different strains of bacteria, which can be related to the different substituents such as hydroxyl, methoxy and *m*-nitro groups present at the *para*-position of the aryl rings. The antibacterial activities of these compounds were also enhanced by the presence of the fused indole moiety.

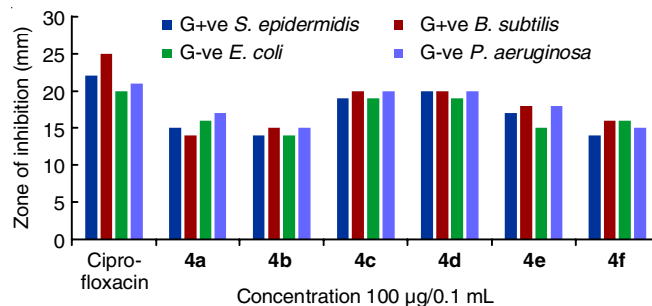


Fig. 6. Antibacterial activity of synthesized compounds **4a-f**

Conclusion

In conclusion, this study explores the synthetic strategy and subsequent chemical transformations of thiazolo-indole hybrid molecules as antimicrobial potential, specifically targeting tuberculosis and bacterial strains. The compounds exhibit promising efficacy, supported by *in silico* toxicity predictions. Molecular docking studies provide insights into their mechanisms of action against infections and antibiotic resistance. This multidisciplinary research, spanning synthesis, evaluation and computational analysis, offers a comprehensive perspective on thiazolo-indoles' potential. These findings inspire future study in developing effective antitubercular and antibacterial agents, addressing urgent challenges in tuberculosis, antibiotic resistance and drug toxicity.

ACKNOWLEDGEMENTS

The authors are grateful to their respective universities for providing materials, chemicals, and reagents. Furthermore, they are also grateful to PASS, Molinspiration, Osiris and Swiss ADME for providing free softwares.

CONFLICT OF INTEREST

The authors declare that there is no conflict of interests regarding the publication of this article.

REFERENCES

- G. Bérubé, *Expert Opin. Drug Discov.*, **11**, 281 (2016); <https://doi.org/10.1517/17460441.2016.1135125>
- S. Short, S. Rhodes, V. Bhave, R. Hojo and M. Jha, *Synthesis*, **51**, 4263 (2019); <https://doi.org/10.1055/s-0039-1690680>
- A. Petrou, M. Fesatidou and A. Geronikaki, *Molecules*, **26**, 3166 (2021); <https://doi.org/10.3390/molecules26113166>
- W.M. Eldehna, M.A. El Hassab, M.F. Abo-Ashour, T. Al-Warhi, M.M. Elaasser, N.A. Safwat, H. Suliman, M.F. Ahmed, S.T. Al-Rashood, H.A. Abdel-Aziz and R. El-Haggar, *Bioorg. Chem.*, **110**, 104748 (2021); <https://doi.org/10.1016/j.bioorg.2021.104748>

5. F. Sachse and C. Schneider, *Adv. Synth. Catal.*, **364**, 77 (2022); <https://doi.org/10.1002/adsc.202101168>
6. M. Konus, D. Çetin, N.D. Kizilkan, C. Yilmaz, C. Fidan, M. Algo, E. Kavak, A. Kivrak, A. Kurt-Kizildogan, Ç. Otur, D. Mutlu, A.H. Abdelsalam and S. Arslan, *J. Mol. Struct.*, **1263**, 133168 (2022); <https://doi.org/10.1016/j.molstruc.2022.133168>
7. D. Lopatik, Z. Kuvaeva, O. Bondareva, V. Naidenov and L. Tychinskaya, *Proc. Natl. Acad. Sci. Belarus, Chemical Ser.*, **55**, 436 (2019); <https://doi.org/10.29235/1561-8331-2019-55-4-436-441>
8. M. Ubeid, H. Thabet and S. El-Feky, *Heterocycl. Commun.*, **22**, 43 (2016); <https://doi.org/10.1515/hc-2015-0135>
9. S.-i. Hattori, N. Higashi-Kuwata, H. Hayashi, S.R. Allu, J. Raghavaiah, H. Bulut, D. Das, B.J. Anson, E.K. Lendy, Y. Takamatsu, N. Takamune, N. Kishimoto, K. Murayama, K. Hasegawa, M. Li, D.A. Davis, E.N. Kodama, R. Yarchoan, A. Wlodawer, S. Misumi, A.D. Mesecar, A.K. Ghosh and H. Mitsuya, *Nat. Commun.*, **12**, 668 (2021); <https://doi.org/10.1038/s41467-021-20900-6>
10. S. Nasri, M. Bayat, H.V. Farahani and S. Karami, *Heliyon*, **6**, e03687 (2020); <https://doi.org/10.1016/j.heliyon.2020.e03687>
11. D.G. Kim and A.V. Zhuravlyova, *Chem. Heterocycl. Compd.*, **45**, 1281 (2009); <https://doi.org/10.1007/s10593-010-0421-5>
12. V.V. Marysheva and P.D. Shabanov, *Bull. Exp. Biol. Med.*, **147**, 55 (2009); <https://doi.org/10.1007/s10517-009-0450-1>
13. S. Sharma, B.M. Sahoo and B.K. Banik, *Lett. Org. Chem.*, **20**, 1016 (2023); <https://doi.org/10.2174/1570178620666230518145740>
14. The TB/COVID-19 Global Study Group, *Eur. Respir. J.*, **59**, 2102538 (2022); <https://doi.org/10.1183/13993003.02538-2021>
15. R. Mangali and S. Muthusamy, *Asian J. Org. Chem.*, **12**, e202300142 (2023); <https://doi.org/10.1002/ajoc.202300142>
16. S. Thakur, R. Sharma, R. Yadav and S. Sardana, *Chem. Proc.*, **12**, 36 (2022); <https://doi.org/10.3390/ecsoc-26-13673>
17. S. Kumar and Ritika, *Future J. Pharm. Sci.*, **6**, 121 (2020); <https://doi.org/10.1186/s43094-020-00141-y>
18. B.F. Abdel-Wahab and H.A. Mohamed, *Phosphorus Sulfur Silicon Rel. Elem.*, **191**, 1199 (2016); <https://doi.org/10.1080/10426507.2016.1160242>
19. N.R. Candeias, L.C. Branco, P.M.P. Gois, C.A.M. Afonso and A.F. Trindade, *Chem. Rev.*, **109**, 2703 (2009); <https://doi.org/10.1021/cr800462w>
20. D.A. Filimonov, A.A. Lagunin, T.A. Glorizova, A.V. Rudik, D.S. Druzhilovskii, P.V. Pogodin and V.V. Poroikov, *Chem. Heterocycl. Compd.*, **50**, 444 (2014); <https://doi.org/10.1007/s10593-014-1496-1>
21. A. Ayar, M. Aksahin, S. Mesci, B. Yazgan, M. Gül and T. Yildirim, *Curr. Computeraided Drug Des.*, **18**, 52 (2022); <https://doi.org/10.2174/1573409917666210223105722>
22. T. Sander, Actelion's Property Explorer, Allschwil, Switzerland: Actelion's Pharmaceuticals Ltd. (2001).
23. A. Daina, O. Michielin and V. Zoete, *Sci. Rep.*, **7**, 42717 (2017); <https://doi.org/10.1038/srep42717>
24. R.A. Friesner, R.B. Murphy, M.P. Repasky, L.L. Frye, J.R. Greenwood, T.A. Halgren, P.C. Sanschagrin and D.T. Mainz, *J. Med. Chem.*, **49**, 6177 (2006); <https://doi.org/10.1021/jm051256o>
25. D. Eisenberg, R. Luthy and J.U. Bowie, *Methods Enzymol.*, **277**, 396 (1997); [https://doi.org/10.1016/S0076-6879\(97\)77022-8](https://doi.org/10.1016/S0076-6879(97)77022-8)
26. C. Colovos and T.O. Yeates, *Protein Sci.*, **2**, 1511 (1993); <https://doi.org/10.1002/pro.5560020916>
27. S. Analysis and V. Server (2011); Available from: <http://nihserver.mbi.ucla.edu/SAVES/>.
28. S.C. Lovell, I.W. Davis, W.B. Arendall 3rd, P.I. de Bakker, J.M. Word, M.G. Prisant, J.S. Richardson and D.C. Richardson, *Proteins*, **50**, 437 (2003); <https://doi.org/10.1002/prot.10286>
29. Chem DrawUltra version 8.0.3 for Windows, Cambridge Soft Corporation, A subsidiary of Perkin-Elmer, Inc. (2014); Available from: www.cambridgesoft.com.
30. <https://sourceforge.net/projects/openbabel/files/openbabel/2.4.0/>. License: GNU GPL v2.
31. N.M. O'Boyle, M. Banck, C.A. James, C. Morley, T. Vandermeersch and G.R. Hutchison, *J. Cheminform.*, **3**, 33 (2011); <https://doi.org/10.1186/1758-2946-3-33>
32. E. Harder, W. Damm, J. Maple, C. Wu, M. Reboul, J.Y. Xiang, L. Wang, D. Lupyán, M.K. Dahlgren, J.L. Knight, J.W. Kaus, D.S. Cerutti, G. Krilov, W.L. Jorgensen, R. Abel and R.A. Friesner, *J. Chem. Theory Comput.*, **12**, 281 (2016); <https://doi.org/10.1021/acs.jctc.5b00864>
33. S.G. Franzblau, R.S. Witzig, J.C. McLaughlin, P. Torres, G. Madico, A. Hernandez, M.T. Degan, M.B. Cook, V.K. Quenzer, R.M. Ferguson and R.H. Gilman, *J. Clin. Microbiol.*, **36**, 362 (1998); <https://doi.org/10.1128/JCM.36.2.362-366.1998>
34. B. Aneja, M. Azam, S. Alam, A. Perwez, R. Maguire, U. Yadava, K. Kavanagh, C.G. Daniliuc, M.M.A. Rizvi, Q.M.R. Haq and M. Abid, *ACS Omega*, **3**, 6912 (2018); <https://doi.org/10.1021/acsomega.8b00582>
35. CLSI, M100 Performance Standards for Antimicrobial Susceptibility Testing, CLSI: Wayne, PA, USA, Edn. 29 (2019).